JOURNAL OF Materials CHEMISTRY

X-ray and optical studies of the tilted phases of materials exhibiting antiferroelectric, ferrielectric and ferroelectric mesophases

Joanne T. Mills,[a] Helen F. Gleeson,*[a] John W. Goodby,[b] Michael Hird,[b] Alexander Seed[b] and Peter Styring[b]

[a] *The Department of Physics and Astronomy, The University of Manchester, Manchester, UK M13 9PL*
[b] *The School of Chemistry, The University of Hull, Hull, UK HU6 7RJ*

Received 20th July 1998, Accepted 2nd September 1998

X-Ray and optical techniques have been employed to probe the physical properties of six materials that exhibit various frustrated chiral smectic phases. The temperature dependent evolution of the layer spacing, measured by small angle X-ray diffraction, is discussed with respect to the molecular structures of the materials. The layer spacings are used to deduce the steric tilt angle of the systems across the ferro-, ferri- and antiferro-electric phase ranges. Measurements of the steric and saturated optical tilt of the phases are compared. In general, for most materials and at most temperatures, the steric tilt is lower than the X-ray tilt as would be expected. However, in three of the materials the X-ray tilt is higher than the optical tilt over part of the high temperature tilted phase regime, providing evidence of conformation driven inversion phenomena. Further, the ratio of the steric to optical tilt angle is strongly temperature dependent in all but two of the materials.

Introduction

The occurrence of antiferroelectric and ferrielectric phases in liquid crystals is well documented,[1] though details of the structures of these phases are still the subject of some debate. The currently accepted structures of the ferroelectric, ferrielectric and antiferroelectric phases have been described in detail elsewhere.[1] Briefly, all the phases include layers in which the director is tilted with respect to the layer normal at a temperature dependent angle. In the ferroelectric phase, all the layers tilt in the same direction, the antiferroelectric structure has alternating layers tilted in opposite directions, while the ferrielectric phases exhibit some proportion of layers tilted in either direction. The existence of antiferroelectricty and ferrielectricity in liquid crystals provides a challenge to both experimentalists and theoreticians who continue to carry out elegant work both deducing the structures and providing theories for their stabilisation. Many of the studies of antiferro- and ferri-electric systems are on the well known material MHPOBC[2] and a variety of experimental techniques have been employed in the task of deducing the structures of the phases exhibited. It is clear that the most useful information is provided when several complementary techniques are used to probe the physical properties of the complex phases and subphases that can occur in antiferroelectric liquid crystals. This paper reports the phase behaviour of six new antiferroelectric materials and describes the behaviour of their tilt as a function of temperature. Two different techniques are employed to deduce the tilt of the systems. Both the optical tilt and the tilt deduced from X-ray layer spacings are reported and compared. The results are interpreted in terms of the conformational structures of the molecules.

Materials

The molecular structures and phase transitions of the materials studied are presented in Fig. 1 and Table 1, respectively. The materials were synthesised at Hull University and their synthesis is reported elsewhere.[3] Fig. 1 shows that the materials studied are structurally similar, including identical terminal chains and chiral centres. The differences between the materials involve substitution on the ring systems. Table 1 shows that

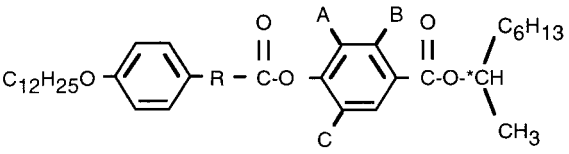

Material	R	A	B	C
AS618	R1	H	H	H
AS661	R1	H	H	F
AS666	R1	H	F	H
AS656	R1	F	F	H
AS620	R2	H	H	H
AS657	R2	F	F	H

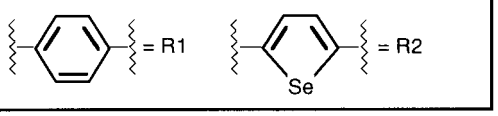

Fig. 1 The structures of the materials studied.

AS661, AS656, AS620 and AS657 all have the same high temperature phase sequence with the SmC* phase occurring directly below the SmA phase. In AS618 there is a SmC^*_α phase intervening between the SmA phase and the SmC* phase. AS666 lacks a SmC* phase exhibiting a direct phase transition from the SmA to a SmC^*_γ phase. AS620 also exhibits a monotropic phase transition to a SmI^*_A phase at 42 °C which is not shown in the Table as it is well below the temperature range of the measurements reported.

The phase behaviour of materials that exhibit ferro-, ferri- and antiferro-electricity is complex and there is still much debate about the subphases that appear in them. The difficulty of identifying various of the mesophases that occur is reviewed by Itoh *et al.*[4] who describe how misidentification occurs as a result of supercooling, phase sequences and surface interactions. For example, the phase sequences reported for AS573 (the opposite enantiomer of AS661)[5–7] are reported to be different according to the techniques employed to study the temperature dependent material properties, though it seems likely that at least two ferrielectric phases and possibly two

Table 1 Phase transition temperatures[a]

	Transition temperature/°C						
Material	K-SmC*$_A$	SmC*$_A$–SmC*$_\gamma$	SmC*$_\gamma$–SmC*	SmC*–SmC*$_\alpha$	SmC*$_\alpha$–SmA	SmC*–SmA	SmA–I
AS618	72.9	99.9	103.5	117.0	122.2		129.3
AS661	53.3	78.3	82.0	—	—	90.7	105.7
AS666	39.6	108.4	—	—	—	118.6 (γ–A)	126.7
AS656	52.8	94.0	95.2	–	–	99.5	110.8
AS620[b]	67.7	97.8	99.0	—	—	109.4	116.6
AS657	46.3	79.7	83.3	—	—	84.3	93.7

[a]No distinction is made between the SmC*$_\beta$ and SmC* phases. The SmC*$_\gamma$ phase encompasses possible subdivisions into other ferrielectric phases. [b]AS620 also exhibits SmI*$_A$ and SmI* phase transitions at 42.2 and 33.3 °C (not shown).

antiferroelectric phases exist in the system. The complex phase behaviour of AS661 and AS573 is the subject of a further publication.[8] In this paper, no distinction is made between the SmC* phase and the SmC*$_\beta$ phase, nor is any subdivision made of the SmC*$_\gamma$ phase into other ferrielectric subphases since the techniques employed for the work reported here do not allow these subphases to be distinguished.

Experimental

The transition temperatures of the materials were determined by optical microscopy and differential scanning calorimetry to within ± 0.2 °C. In the optical experiments the sample was held on a Linkam THMS 600 hot stage and the temperature was maintained with a relative accuracy of ± 0.1 °C using a Linkam TMS 91 control unit. In the X-ray measurements a specially modified Linkam hot stage DSC system was used to control the sample temperature[9] again with a relative accuracy of ± 0.1 °C.

The liquid crystal samples were held in commercially produced[10] devices of nominal thickness 5 μm for the optical tilt angle measurements. The inner surfaces of the devices had been treated with rubbed polyimide to promote antiparallel alignment and the devices included transparent indium tin oxide electrodes to allow the application of electric fields. Alternating fields of up to 40 V μm^{-1} were produced across the device from a signal generator connected to a wide band amplifier constructed in-house. The optical tilt angles of the materials were determined with an accuracy of $\pm 0.5°$ across the mesophase range by observation of the extinction angles of the samples when viewed between crossed polarisers. These experiments were performed using white light on an Olympus polarising microscope. The optical tilt angle of the materials are field dependent due to both the chiral and antiferro- or ferri-electric nature of the materials. Thus, sufficiently large fields (± 10 V μm^{-1}) were applied during the measurements to the samples to ensure that the tilt angle value was saturated. Observation of the samples *via* polarising microscopy during the optical tilt angle measurements ensured that the high fields necessary to ensure saturation did not have the adverse effect of distorting the alignment of the sample, a well known phenomenon that would result in erroneous tilt angle measurements.

X-Ray diffraction was employed to probe the temperature dependent layer spacing of the materials. The small angle X-ray scattering (SAXS) experiments were carried out on station 8.2 of the Synchrotron Radiation Source (SRS), Daresbury, UK. The apparatus has been described in detail elsewhere[11] and includes facilities to perform concurrent DSC and SAXS, allowing the smectic to isotropic phase transition temperatures of the materials to be determined *in situ* with an accuracy of ± 0.5 °C. The X-ray camera was 1.0 m in length, was equipped with an area detector and X-rays of wavelength of 1.54 Å were incident on the sample. The measurements were made on unaligned samples which were held in DSC pans fitted with thin Mylar windows to allow the passage of incident and scattered X-rays with minimal attenuation. The thickness of the liquid crystal sample was approximately 1 mm. The layer spacing in the smectic mesophases was deduced from the position of the first order Bragg scattering peak with an accuracy of 0.5%, which for a layer spacing of 35 Å equates to an uncertainty of ± 0.2 Å. The steric tilt angle δ was deduced from the layer spacing measurements using the equation $\cos \delta = d/l$ where d is the smectic layer spacing and l is the molecular length. The way in which the molecular length was determined is discussed later.

Results and discussion

Layer spacing measurements

The layer spacings of the materials are shown across their mesophase ranges as a function of reduced temperature in Fig. 2. The phase transition from the orthogonal to tilted smectic phases is clear on the figures, occurring at the point

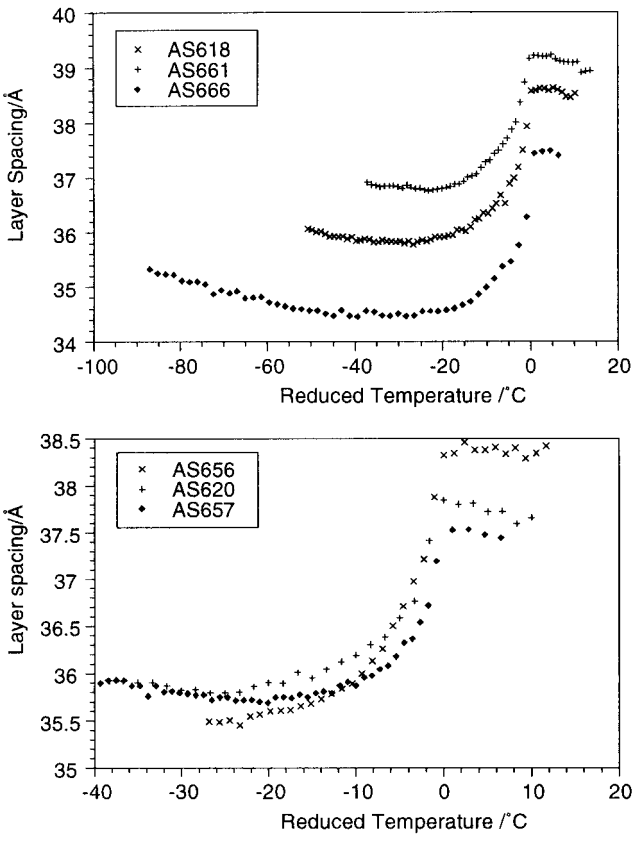

Fig. 2 The layer spacings of the six materials studied as a function of reduced temperature (the temperature below the tilted to orthogonal SmA phase transition).

where the layer spacing reduces dramatically. The temperatures at which this marked change in layer spacing occurs is consistent with the SmA to SmC* (or SmC*$_\alpha$) phase transition temperatures given in Table 1.

In all six of the materials studied, the layer spacing in the SmA phase increases slightly as the temperature is reduced. This observation implies that contraction of the layers does not occur as the temperature decreases, a phenomenon that is common in other SmA systems.[12–14] Several effects could result in a slightly increasing layer spacing with reducing temperature, including changes in the conformation of the alkyl chain or a changing population of the conformers occurring as function of temperature, a suggestion that is supported by further evidence discussed in later sections of this paper.

Comparing the temperature range of the SmC*$_A$ phase in the six materials studied materials to the smectic layer spacings in the antiferroelectric phase leads to the conclusion that a wider SmC*$_A$ range correlates with a smaller layer spacing. This phenomenon has also been observed by Ikeda *et al.*[15] and supports the theory that the molecular pairing believed to occur between adjacent layers in the SmC*$_A$ phase[1] plays an important role in its stabilisation. A greater degree of pairing implies a stronger antiferroelectric attraction between adjacent layers, the stronger attraction resulting in a shorter the layer spacing. Thus a more stable SmC*$_A$ phase would be expected to have a shorter layer spacing.

Below the orthogonal to tilted phase transition, the layer spacings initially decrease rapidly, then change little with temperature as the tilt angles saturate. It can also be seen that at low temperatures, within the SmC*$_A$ phases, the spacings of all the materials increase as the temperature is reduced, an effect that is very marked in AS666. The general trend of layer spacing as a function of temperature is similar to that reported by Rao *et al.* for an antiferroelectric compound with quite different terminal groups.[16] They attributed the increase of layer spacing at lower temperatures in the SmC*$_A$ phase to an underlying SmI*$_A$ phase. The only compound for which that is possible here is AS620 as none of the other materials studied have been observed to exhibit underlying hexagonal phases. Further, the increase in layer spacing in the SmC*$_A$ phase occurs well above the temperature associated with the monotropic phase transitions to the hexagonal smectic phases in AS620. The observed increase in the layer spacing is not reflected in the optical tilt angles, as is shown in a later section, and so cannot be attributed to changes in the director tilt angle. The low temperature increase in layer spacing continues the trend observed in the SmA phase and is likely to be due to increasingly restricted conformational structures and hindered rotation of the molecules as the temperature reduces.

The molecular length

The steric tilt angle δ can be deduced from the layer spacing data using the equation $\cos\delta = d/l$, where d is the layer spacing and l is the molecular length. In order to employ this technique of deducing the steric tilt angle, it is clearly necessary to have a measure of the molecular length l for the materials studied. The simplest method of deducing a value for this parameter is to assume that the layer spacing in the SmA phase is identical to the molecular length, though the validity of such an assumption clearly depends on whether or not the layers are intercalated. It also neglects the temperature dependence of the layer spacing reported in the previous section and assumes that the molecules are in their most extended form in the SmA phase, an assumption which is rarely valid. Table 2 shows the molecular length for each of the materials studied, considered to be the layer spacing at the point at which the orthogonal to tilted phase transition takes place.

An alternative method of deducing the molecular length relies on molecular modelling, which has the advantage of making no assumptions about packing or thermal effects within a mesophase, but can give erroneous results as molecular conformations other than those that actually occur in the mesophase may be modelled. Molecular modelling was undertaken using Cerius[2] on a silicon graphics workstation for one of the materials reported here, AS661. The modelling yielded a molecular length of 39.3 Å (measured from tip to tip of the molecule). This value is only 0.1 Å different from that determined from the layer spacing, implying that the layers are well defined and that there is little or no interpenetration of layers in the SmA phase of AS661. Further, it seems that the molecules are in an almost completely extended configuration in the SmA phase. Given the structural similarities of the materials studied and their molecular lengths (Table 2), it is likely that the remainder of the materials behave in a similar manner.

Table 2 The molecular lengths of the six materials studied, deduced from the layer spacing in the SmA phase

Material	Molecular length/Å
AS 618	38.6±0.1
AS661	39.3±0.1
AS666	37.4±0.1
AS656	38.4±0.1
AS620	37.9±0.1
AS657	37.5±0.1

The molecular lengths given in Table 2 are approximately the same for all of the systems studied. This is not surprising as all the materials have a C12 alkyl chain on one end and a C6 alkyl chain on the other with the same number of atoms across the length of the core. The two materials containing Se atoms, AS620 and AS657, have shorter lengths than all of the others apart from AS666. The selenophene group has been shown previously[17] to promote a bend in the molecule (18° in the core of AS620 relative to a structure containing biphenyl rings) so the shorter molecular lengths AS620 and AS657 are not unexpected.

All of the compounds have an ester linkage between the aromatic rings which will induce some bend into the core. The shortest molecular length is observed for AS666, possibly because of an increased molecular bend caused by repulsion between the fluorine atom and the end ester group near the chiral centre. In AS661, the longest molecule, the fluorine atom is on the opposite side of the molecule to the ethyl group so this phenomenon does not occur. Rather, the inward pointing F atom may repel the ester dipole, straightening the core to some extent and resulting in the longest molecular length.

Tilt angle measurements

Fig. 3(a) to (f) show the optical and steric tilt angles of the materials AS618, AS661, AS666, AS656, AS620 and AS657, respectively. It should be noted that the uncertainty in temperature associated with the two different measurement techniques could translate into offsets of the order of a degree between the data sets plotted on each graph. For all the materials the optical tilt angle θ was greater than the steric tilt angle δ over the majority of the phase range, implying that the molecular cores are more tilted than the terminal alkyl chains. This observation is in keeping with the Wulf model.[18] There is evidence in three of the materials that δ is larger than θ over part of the high temperature tilted phase region, a phenomenon that is discussed in more detail later.

The maximum values of the steric and optical tilt angles attained in the materials are compared in Table 3. The optical tilt angles are all relatively large (around 30°). The two materials containing Se (AS620 and AS657) have significantly lower steric tilt angles than the other compounds. These

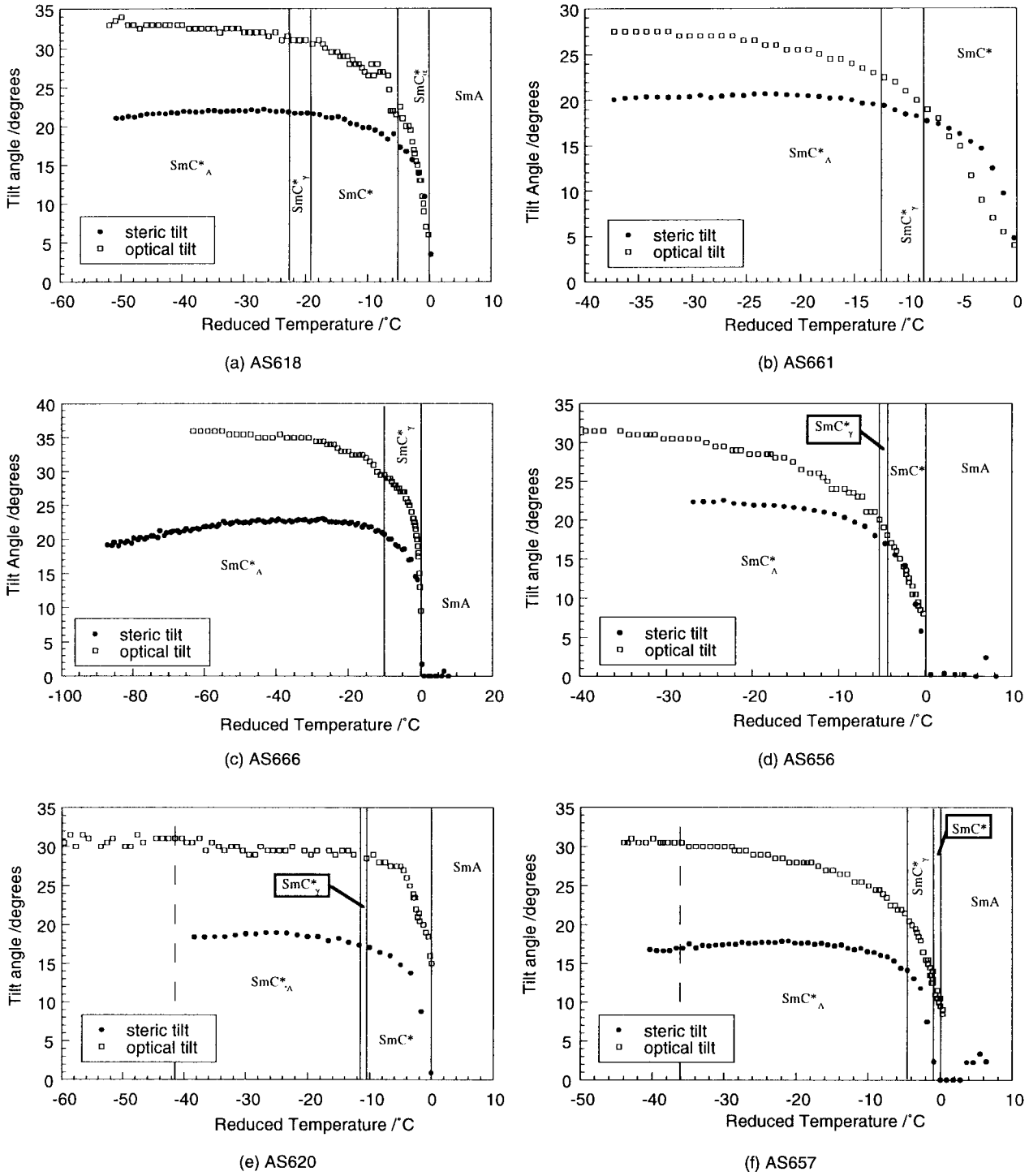

Fig. 3 The steric and optical tilt angles of (a) AS618, (b) AS661, (c) AS666, (d) AS656, (e) AS620 and (f) AS657 as a function of reduced temperature.

Table 3 A summary of the saturated values of the optical tilt angle θ and the steric tilt angle δ

Material	Saturated steric tilt angle δ (°)	Saturated optical tilt angle θ (°)
AS618	21.4	33.0
AS661	20.0	27.7
AS666	21.1	36.1
AS656	22.3	31.4
AS620	18.3	30.6
AS657	16.8	31.1

materials also had amongst the shortest molecular lengths, though the small steric tilt angles cannot be attributed to that factor as it is taken account of in the calculation of δ. Although AS661 is a shorter molecule than AS620 and AS657, it has a larger steric tilt than either, and while δ is still lower than that of the other three materials, the optical tilt of AS661 is also low. It is possible that the small steric tilts of AS620 and AS657 are because the electron dense selenium atom in these systems biases the X-ray tilt to lower values, which could happen if, on average, it remained on the inside of the cone. Such an effect may be the result of hindered rotation about the molecular long axis. Alternatively, packing constraints in the mesophases, imposed due to the molecular bend that is

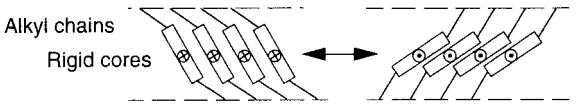

Fig. 4 A schematic diagram of conformational changes in zig-zag molecules that result in inversion phenomena.

known to occur these molecules, could equivalently cause the axis of electron density to appear tilted at a lower angle than would occur for unbent molecules.

The data for AS661 [Fig. 3(b)] clearly show a change from $\delta > \theta$ to $\theta > \delta$ in the middle of the temperature regime identified as a SmC* phase. There is also some evidence of a similar effect in the data for AS618, close to the tilted to orthogonal phase transition. Such an effect is consistent with a conformational change (inversion) occurring in the zig-zag shaped molecules of the sort depicted in Fig. 4.[19–21] Optical observations made of the pitch of this system show inversion phenomena and are reported elsewhere.[8]

It is apparent from Fig. 3(a) to (f) that the temperature dependence of θ and δ appears to be different for some of the materials. In order to investigate the effect further for all of the materials the data were replotted to show the variation of the ratio δ/θ with respect to reduced temperature, as is shown in Fig. 5. It is worth noting when examining the data for the ratio δ/θ that as both δ and θ change rapidly directly below the SmA phase transition, the uncertainty in the ratio is greatest in this region. As mentioned previously, the uncertainty occurs primarily because of the difficulty in registering the absolute temperature measurements in the two different experiments. Consequently, the ratios calculated within 2 °C of the phase transition are discarded and not shown in Fig. 5. In spite of this precaution, it is recognised that the data of Fig. 5 are least reliable in the vicinity of the tilted to orthogonal phase transition.

Rieker *et al.* report that the ratio of δ/θ for a ferroelectric material (not containing antiferroelectric subphases) is almost temperature independent and that $\delta/\theta \sim 0.85$, in common with many ferroelectric materials.[22] The factor of 0.85 is of course material dependent and is determined by the relative orientations of axes of the electron density and polarisability in the system. For the materials described here, it is clear that the ratio can fall within a number of different values, as may be expected from the different degrees of molecular bend in the various systems, together with the inclusion of electron dense selenium atoms in two of the compounds. The ratio δ/θ is almost temperature independent for two of the materials, AS666 and AS620, and takes values of 0.64 and 0.6, respectively. These materials are therefore considered to behave as would be expected for ferroelectric systems. The ratio exhibits a strong temperature dependence for the three of the materials

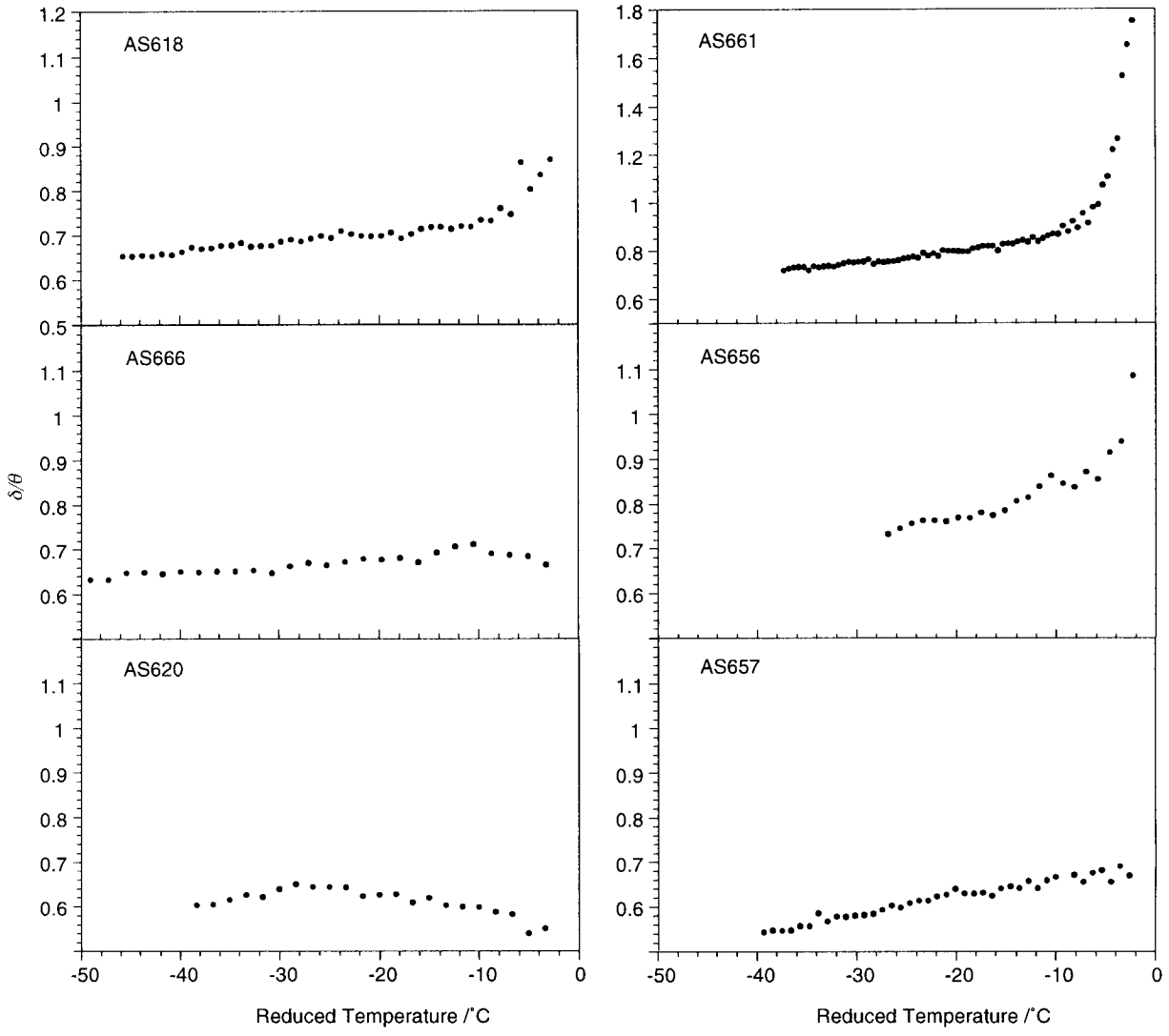

Fig. 5 The ratio of the steric (δ) to optical (θ) tilt angle for the six materials studied. Note that the scales on the graphs corresponding to the value δ/θ is identical for all the materials apart from AS661, where it is significantly different. The temperature scales are identical for all of the graphs, with zero reduced temperature at the orthogonal to tilted phase transition.

studied, AS618, AS661 and AS656, passing through 1 for the latter two. Most of the temperature dependence occurs close to the tilted to orthogonal transition, and is most likely to be attributed primarily to the conformational change depicted in Fig. 4. However, the ratio continues to be temperature dependent well below this transition, in common with the behaviour of the ratio for AS657. We attribute such behaviour to factors other than the zig-zag conformational change, including increasingly restricted conformational structures and hindered rotation of the molecules, as was discussed earlier.

Conclusions

This paper presents layer spacing and tilt angle measurements for six different materials that exhibit ferroelectric and antiferroelectric phases and subphases. The tilt angles were measured both optically and deduced from X-ray layer spacing measurements. Several features are common to all the systems studied. Firstly, the layer spacing measurements in the orthogonal phases imply that the molecules are considerably bent, in common with other systems that exhibit antiferroelectricity. There is evidence that the molecules are almost completely extended in the SmA phase. The layer spacing changes rapidly with temperature at the transition to the tilted phases, as would be expected. The layer spacing reaches a minimum value, then rises again as the temperature is reduced into the antiferroelectric phase. Previous work has attributed such behaviour to underlying SmI^*_A and SmI* phases, though this cannot be the case here, since only one of the materials studied exhibits such a sequence and none of the materials shows any reduction in the optical tilt angle of the system in the range in question. The result must therefore be interpreted as being due to increasingly restricted conformational structures and hindered rotation of the molecules as the temperature reduces.

Comparison of the optical and steric tilt angles shows convincing evidence of inversion behaviour occurring in the regions corresponding to the SmC* phase in three of the materials. Such behaviour has been confirmed by independent measurements of the pitch for AS661. It should be noted that the phase behaviour of these materials, in particular AS661, is the subject of considerable debate. Certainly inversion behaviour, in addition to the other factors mentioned previously, further complicates the phase identification process. In particular, inversion behaviour will be important in many of the measurements currently employed to distinguish the SmC^*_β phase from the SmC* phase as it will affect electroclinic[23] and dielectric relaxation phenomena.[7] This phenomenon will be the subject of a future publication.[24]

The authors gratefully acknowledge the support of the EPSRC (through grant number GR/L/76648) and the DERA Displays Group, Malvern. Thanks are also due to Dr B. Komanschek of Station 8.2 at Daresbury Laboratories, UK, for his help during the XRD work.

References

1 See for example: A. Fukuda, Y. Takanishi, T. Isozaki, K. Ishikawa and H. Takezoe, *J. Mater Chem.*, 1994, **4**, 997; A. D. L. Chandani, E. Gorecka, Y. Ouchi, H. Takezoe and A. Fukuda, *Jpn. J. Appl. Phys.*, 1989, **28** L1265; A. Ikeda, Y. Takanishi, H. Takezoe and A. Fukuda, *Jpn J. Appl Phys.*, 1993, **32** L97.
2 A. D. L. Chandani, Y. Ouchi, H. Takezoe and A. Fukuda, *Jpn. J. Appl. Phys.*, 1989, **28**, L1261.
3 M. Hird, P. Styring, A. Seed, H. F. Gleeson and J. T. Mills, unpublished work.
4 K. Itoh, M. Kabe, K. Miyachi, Y. Takanishi, K. Ishikawa, H. Takezoe and A. Fukuda, *J Mater. Chem.*, 1997, **7**, 407.
5 J. W. Goodby and I. Nishiyama, unpublished DSC data.
6 W. K. Robinson, PhD Thesis, Manchester University, Manchester, UK, 1995.
7 Y. Panarin, W. Kalinovskaya, J. K. Vij and J. W. Goodby, *Phys Rev. E*, 1997, **55**, 4345.
8 L. Baylis, unpublished work.
9 W. Bras, G. E. Derbyshire, A. J. Ryan, J. Cooke, A. Devine, B. E. Komanschek and S. M. Clark *J. Appl. Crystallogr.*, 1995, **28**, 26.
10 Lucid EEV, 106, Waterhouse Lane, Chelmsord, Essex, UK CM1 2QU.
11 W. Bras, G. E. Derbyshire, A. J. Ryan, G. R. Mant, A. Felton, R. Lewis, C. Hall and N. Greaves, *NIM*, 1993, **587**, A326.
12 J. Stamatoff, P. E. Cladis, D. Guillion, M. C. Cross, T. Bilash and P. Finn, *Phys. Rev. Lett.*, 1980, **44**, 1509.
13 Y. Ouchi, Y. Takanishi, H. Takezoe and A. Fukuda, *Jpn. J. Appl. Phys.*, 1989, **28**, 2547.
14 A. S. Morse and H. F. Gleeson, *Liq. Cryst.*, 1997, **23**, 531.
15 A. Ikeda, Y. Takanishi, H. Takezoe and A. Fukuda, *Jpn. J. Appl. Phys.*, 1993, **32**, L97.
16 D. S. S. Rao, S. K. Prasad, S. Chandrasekhar, S. Mery and R. Shashidhar, *Mol. Cryst. Liq. Cryst.*, 1997, **292**, 301.
17 J. T. Mills, R. J. Miller, H. F. Gleeson, A. J. Seed, M. Hird and P. Styring, *Mol. Cryst. Liq. Cryst.*, 1997, **303** 145.
18 A. Wulf, *Phys. Rev. A*, 1975, **11**, 365.
19 J. S. Patel and J. W. Goodby, *Philos. Magazine Lett.*, 1987, **55**, 283.
20 J. S. Patel and J. W. Goodby, *J. Phys. Chem.*, 1987, **91**, 5838.
21 J.-H. Kim, S.-D. Lee, J. S. Patel and J. W. Goodby, *Mol. Cryst. Liq. Cryst.*, 1994, **247**, 293.
22 T. P. Rieker, N. A. Clark, G. S. Smith, D. S. Parmar, E. B. Sirota and C. R. Safinya, *Phys. Rev. Lett.*, 1987, **59**, 2658.
23 T. Sako, Y. Kimura, R. Hayakawa, N. Okabe and Y. Suzuki, *Jpn. J. Appl. Phys.*, 1996, **35**, L114.
24 H. F. Gleeson, unpublished work.

Paper 8/05611K